Available online at www.sciencedirect.com

ScienceDirect

Energy Procedia 114 (2017) 302 – 308

Energy Procedia

13th International Conference on Greenhouse Gas Control Technologies, GHGT-13, 14-18 November 2016, Lausanne, Switzerland

Evaluation of $(Mn_xFe_{1-x})_2Ti_yO_z$ particles as oxygen carrier for Chemical Looping Combustion

María Abián, Alberto Abad*, María T. Izquierdo, Pilar Gayán, Luis F. de Diego, Francisco García-Labiano, Juan Adánez

Instituto de Carboquímica (ICB-CSIC), Miguel Luesma Castán, 4, Zaragoza, E-50018, Spain

Abstract

The present work accomplishes a screening of the performance of Mn-Fe-Ti based oxygen carriers, prepared with different Mn/(Mn+Fe) molar ratios in the general formula $(Mn_yFe_{1-y})Ti_{0.15}O_x$. The oxygen carriers were prepared by physical mixing followed by pelletizing under pressure, calcining, crushing and sieving in the 100-300 μm particle size interval. The characterization of the carriers is based on the evaluation of their crushing strength, magnetic properties and reduction and oxidation behavior through TGA experiments at temperatures suitable for the CLC process (i.e. 850-950 ºC). In addition, the main chemical structures of the Mn-Fe-Ti system were identified as a function of the Mn/(Mn+Fe) molar ratio. Oxygen uncoupling property was analyzed by reduction under a N_2 atmosphere and the capability to interact with fuel gases was analyzed by using CH_4, H_2 and CO.

Results indicate that the $(Mn_yFe_{1-y})Ti_{0.15}O_x$ oxygen carriers with Mn/(Mn+Fe) molar ratios of 0.55-0.87 have very promising properties for the CLC process with solid fuels.

Peer-review under responsibility of the organizing committee of GHGT-13.

Keywords: CO_2 capture; CLC; CLOU; Manganese ferrites; Coal.

* Corresponding author. Tel.: +34-976-733-977; fax: +34-976-733-318.
E-mail address: abad@icb.csic.es

Peer-review under responsibility of the organizing committee of GHGT-13.
doi:10.1016/j.egypro.2017.03.1171

1. Introduction

Chemical Looping Combustion (CLC) is an interesting CO_2 capture technology devoted to offer lower capture cost and efficiency penalty than the classic CO_2 capture systems [1]. The Chemical Looping Combustion technology implies the use of an oxygen carrier that circulates between a fuel and an air fluidized bed reactors. This way, the oxygen carrier transfers the oxygen from one to another reactor avoiding the direct contact between fuel and air [2]. There are two approaches for the use of the CLC technology with solid fuels: the *in-situ* Gasification Chemical Looping Combustion (*i*G-CLC) and the Chemical Looping with Oxygen Uncoupling (CLOU) [3]. Oxygen carriers with the capability to release gaseous oxygen in contact with the fuel are required for CLOU. In both *i*G-CLC and CLOU with coal, the generation of ash is, in general, inherent to the solid fuel combustion. Consequently, ash is drained to avoid its accumulation in the unit; and some oxygen carrier particles are also removed within the ash. The lost particles have to be replaced with new material. Thus, low-cost oxygen carriers have been considered for CLC. However, oxygen carriers for CLOU are generally synthetic materials, making them more expensive than minerals commonly used in *i*G-CLC. To reduce the cost of the oxygen carrier makeup, the oxygen carrier separation from ashes is required to be reintroduced in the system.

Mixed oxides of Mn-Fe have been identified as suitable materials for CLC having the property of release oxygen under given conditions, while cheap metals are used [4]. The Mn-Fe system has been considered in previous works (i.e. [5-8]), analyzing the influence of the Mn:Fe ratio on both, its chemical properties (reactivity and capability for releasing oxygen), and its mechanical strength. Main results from these studies indicate that the selection of the ideal Mn-Fe composition will depend on the specific operating conditions [8]. In general, for low temperatures (850ºC) oxygen carriers with high Mn:Fe ratios show better gas conversions and CLOU properties than oxygen carriers with low Mn:Fe ratios, and vice-versa for higher temperatures (900ºC and upper) [5].

In addition, the Mn-Fe mixed oxides can show magnetic properties that could be used for their easy separation from ash. In this sense, different cations such as Ti^{4+} have been proposed to improve the magnetic properties of manganese ferrites [9].

In this context, the present work accomplishes a screening of the performance of Mn-Fe-Ti based oxygen carriers, prepared with different Mn/(Mn+Fe) molar ratios. In particular, the crushing strength, magnetic properties and redox reactivity through TGA experiments are the main characteristics considered in this study.

The thermodynamic properties of the different $(Mn_yFe_{1-y})Ti_{0.15}O_x$ oxygen carrier, and consequently their performance in the CLC system, are conditioned by the specific structural composition of the particles. Figure 1 shows the theoretical stable phases predicted by thermodynamics (FToxid database from the FactSage software [10]) as function of different Mn/(Mn+Fe) molar ratios in the $(Mn_yFe_{1-y})Ti_{0.15}O_x$ system and temperature in an atmosphere with an O_2 partial pressure of 0.05 atm.

In the $(Mn_yFe_{1-y})Ti_{0.15}O_x$ system, low temperature regions are dominated by bixbyite (B) phases, while spinel (S) phase appear in the high temperature region. The temperature for the bixbyite (B) to spinel (S) transformation monotonically decreases as the Mn/(Mn+Fe) ratio increases. In the lower temperature regions, the hematite Fe_2O_3 and rutile TiO_2 phases dominate the regions with lower Mn content, whereas for higher Mn/(Mn+Fe) ratios bixbyte (B) and rutile (R) structures are the main phases present. At higher temperatures, rutile (R) and β-spinel (S) structures predominates in the regions with lower Mn content, whereas pyrophanite (P) and tetragonal spinel (S) gain importance as the Mn/(Mn+Fe) ratio increases. Between the regions dominated by bixbyite and spinel phases, there is a miscibility gap where both phases co-exist. These theoretical stable phases predicted by thermodynamics are compared to solid phases found after characterization of the oxygen carriers by XRD.

For the CLOU system, the oxygen release in the fuel reactor is typically produced from the transformation of bixbyite (B) to spinel (S) structure, and, as already indicated, in this system, the temperature for the bixbyite (B) to spinel (S) transformation decreases as the Mn content is increased. However, based on the phase diagram of Figure 1, when Ti is present in the mixture, oxygen uncoupling can be also produced from the transformation of spinel to pyrophanite structure. Pyrophanite is favoured at high Mn content.

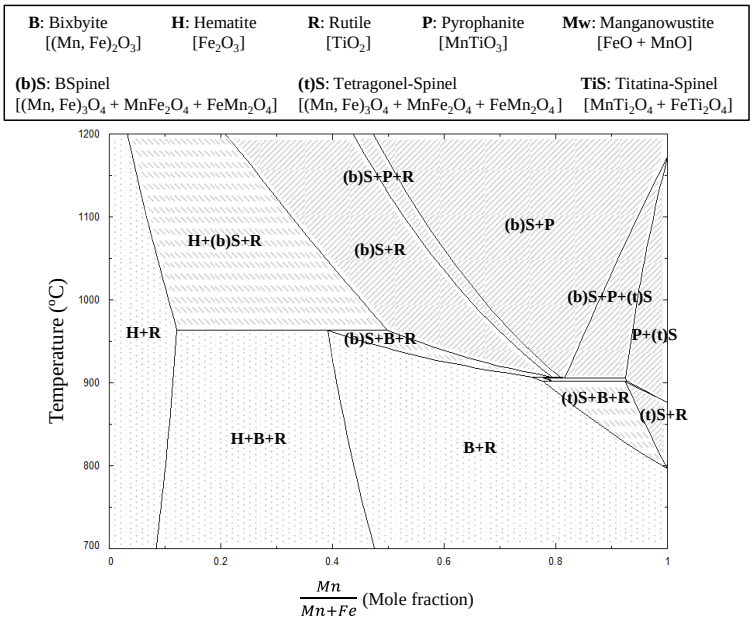

Figure 1. Phase diagram of the $(Mn_yFe_{1-y})Ti_{0.15}O_x$ system as function of the Mn-Fe composition and temperature in an atmosphere with an O_2 partial pressure of 0.05 atm.

Considering these observations, the redox reactivity of the different oxygen carriers has been evaluated through TGA experiments at temperatures of interest for the *i*G-CLC and CLOU process (i.e. 850-950 ºC), using: i) an inert N_2 atmosphere to analyze the oxygen uncoupling behavior; ii) CH_4, H_2 and CO to analyze the possible gas-solid reactions; and iii) an air atmosphere to evaluate their regeneration capability.

2. Experimental

The oxygen carrier particles were prepared using as raw materials powders of Mn_3O_4 (Strem Chemical, Inc), Fe_2O_3 (Panreac, Prs), and TiO_2 (Panreac, Prs). All the oxygen carries contain a fixed TiO_2 concentration of 7 % in weight, and different Mn_3O_4/Fe_2O_3 ratios, ranging from Mn_3O_4 = 100 wt. % to Fe_2O_3 = 100 wt. %. The specific Mn-Fe composition in the different $Mn_xFe_{1-x}Ti_yO_z$ systems has been stablished to cover a wide range of Mn/(Mn+Fe) ratios on the basis of the phase diagram results shown in Figure 1. The given composition of the different oxygen carriers prepared and studied in this work is summarized in Table 1.

To prepare the oxygen carriers, the reactants were mixed in a ball-mill for 2 h and pelletized under pressure at 160 bar for 60 s in a hydraulic press, obtaining cylindrical pellets of about 3 cm in length and 1 cm in diameter. The pellets were calcined at 1200ºC in a muffle furnace during 2 hours and subsequently crushed in a ceramic mortar and sieved in the 100 – 300 μm particle diameter interval. All the oxygen carriers prepared in this work, following this methodology, showed high enough crushing strength (higher than 3.75 N), but not always exhibited magnetic properties; see Table 1. Therefore, in some cases (i.e. Mn87FeTi7), to provide the oxygen carrier particles with magnetic properties, calcination at higher temperatures was necessary. For a detailed description of the magnetic properties and behavior of the oxygen carriers, see [11]. The crushing strength values did not show a direct relation with the Fe content of the $(Mn_yFe_{1-y})Ti_{0.15}O_x$ particles.

Considering the magnetism results, the FeTi7_1200, Mn28FeTi7_1200, Mn55FeTi7_1200, Mn66FeTi7_1200, Mn87FeTi7_1300 and MnTi7_1200 samples were subjected to the reactivity tests, and from now they will be directly referred as: FeTi7, Mn28FeTi7, Mn55FeTi7, Mn66FeTi7, Mn87FeTi7, MnTi7.

The main phases identified by XRD for the different oxygen carriers are in agreement with the predicted phases by thermodynamic calculations (i.e. Figure 1).

Table 1. Chemical composition, calcination temperature, crushing strength and magnetization of the oxygen carriers.

Oxygen carrier(1*)	Mn/(Mn+Fe) molar ratio	Mass fraction Mn_3O_4:Fe_2O_3:TiO_2	Crushing strength(2*) (N)	Magnetism(3*)	Main phases(4*)	R^{ou}_{OC}(5*)	R^{t}_{OC}(6*)
FeTi7_1200	0.00	0:93:7	3.76	NO	Fe_2O_3 Fe_2TiO_4	0	4
Mn28FeTi7_1200	0.28	25:68:7	5.75	YES	$Mn_{1.03}Fe_{1.97}O_4$ Mn_2FeO_4 Fe_2O_3 $Fe_{1.5}Ti_{0.5}O_3$	0.47	4.80
Mn55FeTi7_1200	0.55	50:43:7	4.32	YES	Mn_2FeO_4 $Mn_3Fe_3O_8$ Fe_2TiO_4	1.47	7.30
Mn66FeTi7_1200	0.66	60:33:7	3.79	YES	Mn_2FeO_4 $Mn_{1.58}Fe_{1.42}O_4$ Fe_2TiO_4	1.30	7.40
Mn87FeTi7_1200 _1300 _1350 _1400	0.87	80:13:7	4.67 4.39 4.47 5.45	NO YES YES YES	Mn_2FeO_4 Mn_3O_4 $FeTiO_4$	1.88	7.80
MnTi7_1200 _1400	1.00	93:0:7	5.14 4.77	NO NO	Mn_2O_3 Mn_3O_4 $MnTiO_3$	0.38	6.20

(1*) The nomenclature shows the stoichiometric coefficient x and y in the general formula $Mn_xFe_{1-x}Ti_yO_z$, and the calcination temperature of the particles (°C).

(2*) The crushing strength of the particles was measured using a Shimpo FGN-5X crushing strength apparatus.

(3*) The magnetism was qualitatively tested using a magnet.

(4*) The XRD analysis was performed using a Bruker D8 Advance X-ray powder diffractometer with an energy-dispersive one-dimensional detector.

(5*) R^{ou}_{OC} is the effective oxygen transport capacity for oxygen uncoupling at 950°C.

(6*) R^{t}_{OC} is the total oxygen transport capacity for gas-solid reactions at 950°C, including oxygen uncoupling.

The reactivity tests were performed in a *CI Electronics* thermogravimetric analyzer (TGA). The general detailed description of this TGA and the procedure followed to perform the experiments can be found in [12]. The particular experimental conditions for each test include: around 50 mg of oxygen carrier particles and the exposure of the oxygen carrier to three successive reduction-oxidation cycles, with a reaction time of 30 min for either reduction or oxidation period at a fixed temperature. The capability of the different oxygen carriers for release oxygen gas was analyzed by reduction in a 100 % N_2 atmosphere and for interaction with fuel gases was analyzed by using: 15 % CH_4 + 20 % H_2O, 5 % H_2 + 40 % H_2O and 15 % CO + 20 % CO_2 in the reduction period. An air atmosphere was used for the oxidation period.

3. Results and discussion

As a first approach to examine the performance of each oxygen carrier in the CLC process, the normalized oxygen carrier conversion was calculated using Equation 1 for the reduction reaction (X_{red}) and Equation 2 for the oxidation reaction (X_{ox}):

$$X_{red} = \frac{m_o - m}{R^i_{OC,th}\, m_{oxid}} \quad (1)$$

$$X_{ox} = \frac{m - m_r}{R^i_{OC,th}\, m_{oxid}} \quad (2)$$

m_o being the initial mass of the oxygen carrier, m_r the mass of the reduced oxygen carrier, m_{oxid} the mass of the oxygen carrier assuming full oxidation at a defined condition, m the mass of the oxygen carrier at any time and $R^i_{OC,th}$ the mass fraction of the oxygen carrier that can be theoretically transferable as oxygen. For the oxygen uncoupling reaction $R^i_{OC,th} = R^{ou}_{OC,th}$ and it is defined for the reduction of bixbyite to spinel and/or for the reduction of spinel to pyrophanite when required. For reduction with a fuel gas $R^i_{OC,th} = R^t_{OC,th}$ and it is defined for the reduction of bixbyite to manganowüstite.

The evaluation of the oxygen carrier reactivity as function of the reaction temperature has been performed with CH_4 as reduction gas and air as oxidation gas, at 850, 900 and 950 ºC in TGA. Figure 2 shows the normalized oxygen carrier conversion vs. time curves during their reduction with CH_4 and oxidation with air at the different reaction temperatures.

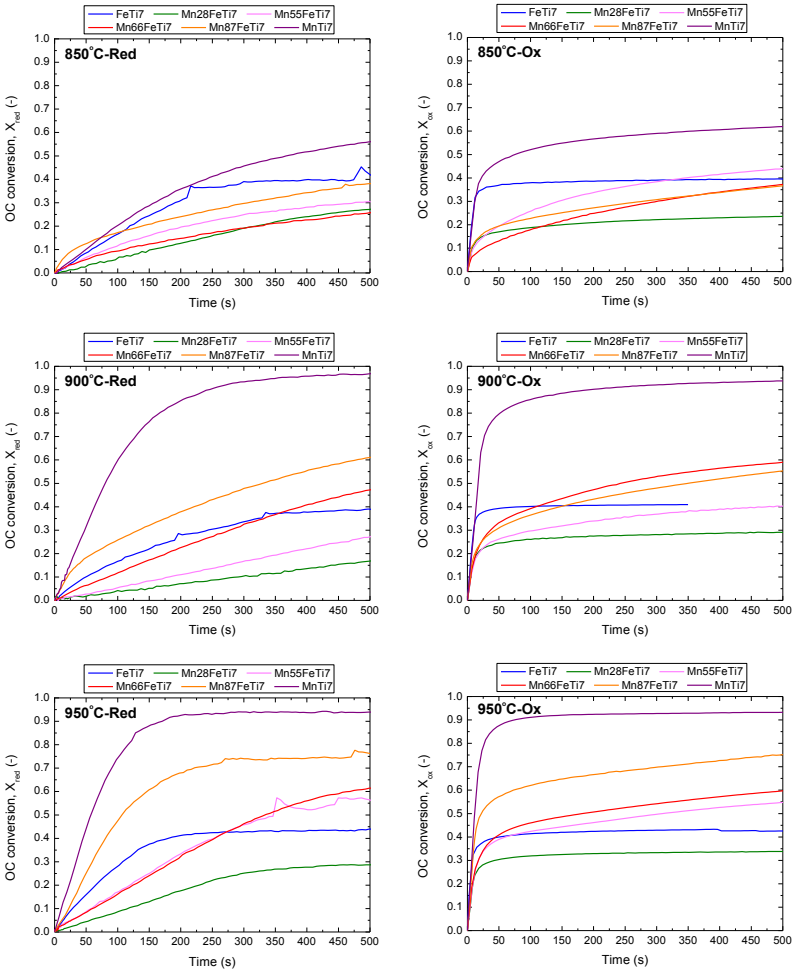

Figure 2. Oxygen carrier particles conversion vs. time during their reaction with CH_4 and air, respectively, at 850, 900 and 950ºC.

These results show that for low Mn content, (Mn/Mn+Fe) molar ratio of 0.28-0.66, the reaction temperature has a low influence on the reduction rate of the oxygen carrier. However, for higher Mn content (i.e. Mn87FeTi7 and MnTi7), the effect of temperature on the oxygen carrier reactivity increases. In fact, for Mn87FeTi7 and MnTi7, the oxygen carrier conversion is considerably promoted when the reaction temperature shifts from 850 to 950°C. The same tendency with temperature can be observed in the reaction with oxygen (reoxidation stage). Therefore for a good performance of this Mn-Fe-Ti system higher temperatures (≥900°C) would be needed in the fuel reactor.

The evaluation of the reactivity of the oxygen carriers with H_2, CO and CH_4, as well as their potential for oxygen release has been performed at 950 ºC. In a first place the CLOU property is evaluated. Figure 3 shows the normalized oxygen carrier conversion vs. time curves during their decomposition in N_2 and reoxidation in air at 950ºC. The FeTi7 carrier is not included in this Figure since, in the absence of a reducing gas, it does not show any phase transformation of interest (see Figure 1).

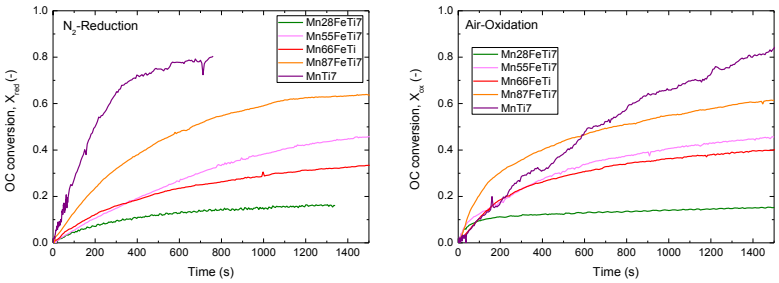

Figure 3. Oxygen carrier particles conversion vs. time during oxygen uncoupling in N_2 atmosphere, and oxidation in air at 950 ºC.

In general, both the oxygen release rate and the maximum carrier conversion are increased as the Mn concentration in the oxygen carrier is increased. However, independently on the Mn/(Mn+Fe) molar ratio, none of the oxygen carriers reach the 100 % conversion and consequently they do not attain the entire useful transport oxygen capacity at this temperature (950ºC).

The results for the interaction of the $(Mn_yFe_{1-y})Ti_{0.15}O_x$ oxygen carriers with fuel gases and their potential to be reoxidated with air is considered as follows. Figure 4 shows the normalized oxygen carrier conversion vs. time curves during their reduction with H_2, CO and CH_4 and reoxidation in air at 950ºC.

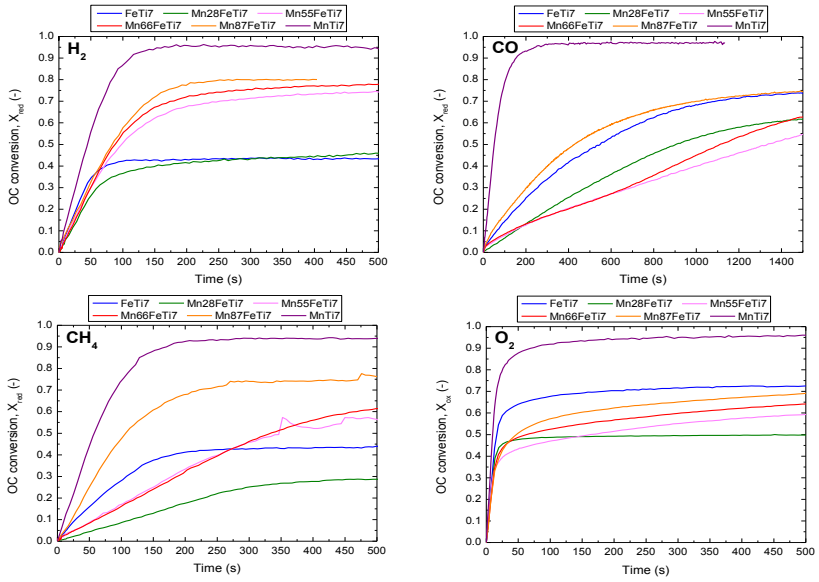

Figure 4. Oxygen carrier particles conversion with time during reduction with: a) 5% H_2 + 40% H_2O, b) 15% CO + 20% CO_2 and c) 15% CH_4 + 20% H_2O, and oxidation with: d) air, at 950 ºC.

For all the oxygen carriers analyzed in this work, the rate of reduction with H_2 is much faster than that with CO and CH_4, regardless the concentration of CO and CH_4 is three times higher than for H_2. Considering a given reduction gas, the degree and rate of the oxygen carrier conversion depends on the given Mn/(Mn+Fe) molar ratio. With the exception of the FeTi7 oxygen carrier, in general, the decrease in the Mn content results into lower degrees and rates of conversion.

In relation to the oxidation process, for all the carriers, a conversion of around 0.4 is reached within the first 20 second of the oxidation period, which points to their capability to be regenerated under these conditions.

4. Conclusions

All the oxygen carriers of the $(Mn_yFe_{1-y})Ti_{0.15}O_x$ system prepared and analyzed in this work show crushing strength values higher than 3.75 N, without direct correlation between the Fe content and the crushing strength values. With the exception of MnTi7 and FeTi7 (i.e. the not combined Mn and Fe oxides), the rest of oxygen carriers developed magnetic properties after their calcination at high temperatures.

Considering the trade-off between kinetics and thermodynamics of the $(Mn_yFe_{1-y})Ti_{0.15}O_x$ system, experimental results reveal that, in general, temperatures $\geq$ 900°C would be needed for a good performance of the materials.

In relation to the results from the reactivity screening at 950ºC, the Mn-Fe-Ti based oxygen carriers with molar ratios in the 0.55-0.87 interval showed either, interesting oxygen uncoupling properties and reactivity behavior with reduction gases (CH_4, H_2 and CO), while a magnetic oxygen carrier is used. Thus, these carriers would be suitable for CLC process with solid fuels due to their specific properties.

Acknowledgments

This work was partially supported by the Spanish Ministry for Economy and Competitiveness via the ENE2013-45454-R project, by the European Regional Development Fund (ERDF), and by the CSIC via the 2014-80E101 project. M. Abián acknowledges the MINECO and Instituto de Carboquímica (ICB-CSIC) for the post-doctoral grant awarded (FPDI-2013-16172).

References

[1] Mukherjeea S, Kumara P, Yangb A, Fennell P. Energy and exergy analysis of chemical looping combustion technology and comparison with pre-combustion and oxy-fuel combustion technologies for CO_2 capture. J Environ Chem Eng 2015;3:2104-2114.

[2] Lyngfelt A, Leckner B, Mattisson T. A fuidized-bed combustion process with inherent CO_2 separation; application of chemical-looping combustion. Chem Eng Sci 2001;56:3101-3113.

[3] Adánez J, Abad A, Garcia-Labiano F, Gayan P, De Diego L.F. Progress in chemical-looping combustion and reforming technologies. Prog Energy Combust Sci 2012;38:215-282.

[4] Rydén M, Leion H, Mattisson T, Lyngfelt A. Combined oxides as oxygen-carrier material for chemical-looping with oxygen uncoupling. Appl Energy 2014;113:1924-1932.

[5] Azimi G, Leion H, Rydén M, Mattisson T, Lyngfelt A. Investigation of different Mn-Fe oxides as oxygen carrier for Chemical-Looping with Oxygen Uncoupling (CLOU). Energy Fuels 2013;27:367-377.

[6] Lambert A, Delquié C, Clémeneçon I, Comte E, Lefebvre V, Rousseau J, Durand B. Synthesis and characterization of bimetallic Fe/Mn oxides for chemical looping combustion. Energy Procedia 2009;1:375-381.

[7] Bhavsar S, Tackett B, Veser G. Evaluation of iron- and manganese-based mono- and mixed-metallic oxygen carriers for chemical looping combustion. Fuel 2014;136:268–279.

[8] Larring Y, Braley C, Pishahang M, Andreassen KA, Bredesen R. Evaluation of a mixed Fe−Mn oxide system for Chemical Looping Combustion. Energy Fuels 2015;29:3438-3445.

[9] Mostafa NY, Hessien MM, Shaltout AA. Hydrothermal synthesis and characterizations of Ti substituted Mn-ferrites. J Alloys Compd 2012;529:29-33.

[10] Bale CW, Bélisle E, Chartrand P, Decterov SA, Eriksson G, Hack K, Jung I-H, Kang Y-B, Melançon J, Pelton AD, Robelin C, Petersen S. FactSage thermochemical software and databases – recent developments. CALPHAD 2009;33:295-311.

[11] Abián M, Abad A, Izquierdo MT, Gayán P, de Diego LF, García-Labiano F, Adánez J. Magnetic oxygen carriers based on titanium substituted manganese-ferrites for Chemical Looping Combustion. Fuel 2016; in the process of submission for publication.

[12] de Diego LF, Abad A, Cabello A, Gayán P, García-Labiano F, Adánez J. Reduction and oxidation kinetics of a $CaMn_{0.9}Mg_{0.1}O_{3-\delta}$. Ind Eng Chem Res 2014;53:87-103.